Available online at www.elixirpublishers.com (Elixir International Journal)

Computational Chemistry

Elixir Comp. Chem. 44 (2012) 7341-7346

ISSN: 2229-712X

Density Functional Theory studies on the structure and vibrational assignments of N, N-Dimethylaniline

G.Raja[a], K.Saravanan[b] and S.Sivakumar[c,*]

[a]Department of Chemistry, Paavai Engineering College, Namakkal-637 018, India.

[b]Department of Chemistry, Thiruvalluvar Government Arts College, Rasipuram-637 401, India

[c]Department of Physics, Arignar Anna Government Arts College, Attur-636 121,India.

ARTICLE INFO

Article history:

Received: 18 January 2012;

Received in revised form:

4 March 2012;

Accepted: 15 March 2012;

Keywords

Normal coordinate analysis,

FT-IR and FT-Raman spectra,

Density functional theory,

First-order hyperpolarizability.

ABSTRACT

The FT-IR and FT-Raman spectra of the N, N-Dimethylaniline (NNDMA) was recorded in the range 4000–400 cm^{-1} and 3500–100 cm^{-1}, respectively. Theoretical information on the optimized geometry, harmonic vibrational frequencies, Infrared and Raman intensities were obtained by means of density functional theory (DFT) using standard B3LYP/6-311++G** level. This information was used in the assignment of the various fundamentals. Comparison of the simulated spectra with the experimental spectra provides important information about the ability of the computational method to describe the vibrational modes.

Introduction

N,N-Dimethylaniline (NNDMA) is an organic chemical compound, a substituted derivative of aniline. It consists of a tertiary amine, featuring dimethylamino group attached to a phenyl group. This oily liquid is colourless when pure, but commercial samples are often yellow. It is an important precursor to dyes such as Crystal violet. NNDMA is a key precursor to commercially important triarylmethane dyes such as Malachite green and Crystal violet. NNDMA serves as a promoter in the curing of polyester and vinyl ester resins. NNDMA is also used as a precursor to other organic compounds.

A number of studies have been carried out regarding the calculations of vibrational spectra using B3LYP methods with the 6-311++G** basis set. As a result, it was found that the experimental vibrational frequencies and IR intensities could be reported very accurately. The scaling factor was applied successfully to the B3LYP method and found to be easily transferable to a number of molecules. Thus vibrational frequencies calculated using the B3LYP function with 6-311++G** as the basis set can be utilized to eliminate the uncertainties in the fundamental assignment in the IR spectra. Accurate vibrational assignments for compound are necessary for characterization of materials. The vibrational assignments at the compounds can be proposed on the basis of wave number agreement between computer harmonics and observed fundamental. The density functional theory has proven to be an essential tool for interpretation and predicting vibrational spectra [1,2].

Experimental Details

The compound NNDMA was purchased from Lancaster Chemical Company USA, with a stated purity of 99% and it was used as such without further purification. The FT-Raman spectrum of NNDMA was recorded using 1064nm line of Nd:YAG laser as excitation wave length in the region 3500–100cm^{-1} with FT-Raman module accessory. The FT-IR spectrum of the title compound was recorded in the region 4000–400cm^{-1} on Perkin Elmer Spectrophotometer. The spectrum was recorded at room temperature with a scanning speed of 30 $cm^{-1}min^{-1}$ and the spectral width of 2.0 cm^{-1}. The observed experimental FT-IR and FT-Raman spectra and theoretically predicted IR and Raman spectra at DFT and B3LYP levels are shown in Fig.1 and 2, respectively.

Computational methods

All the calculations were performed using the 3-parameter hybrid functional (B3) for exchange part and the Lee-Yang-Parr (LYP) [3] correlation function, with 6-311++G** as the basis set using the Gaussian 03 suite of program. The basis set 6-311++G** is a triple–split valance basis set that increases the flexibility of the valence electrons. It is useful for the most studies involving medium–size system. DFT calculations were reported to provide excellent vibrational frequencies of organic compound if the calculated frequencies are scaled to compensate for the approximate treatment of electron correlations, for basis set deficiencies, and for anharmonicity.

The vibrational modes were assigned by means of visual inspection using the GAUSS VIEW program. The analysis for the vibrational modes of NNDMA is presented in some detail in order to better describe the basis for the assignments. From the basic theory of Raman scattering Raman activities (S_i) calculated by Gaussian 03 program have been converted to relative Raman intensities (Ii) using the following relationship:

$$I_i = \frac{f(\nu_o - \nu_i)^4 S_i}{\nu_i\left[1-exp\left(\frac{-hc\nu_i}{KT}\right)\right]} \qquad (1)$$

Where ν_o is the exciting wave number (in cm^{-1} units), ν_i is the vibrational wave number of the in i^{th} normal mode, h, c, and k are universal constant and f is the suitably chosen common scaling factor for all the peak intensities.

Tele:

E-mail addresses: genuineraja@gmail.com

Result and Discussion

Geometrical Structure

The molecular structure of NNDMA having C_s point group symmetry. The most optimized geometry is performed at B3LYP/6-311++G** basis set of NNDMA molecule with atoms numbering scheme shown in Fig.3. The optimized bond length and bond angles of the title compound which are calculated using DFT (B3LYP) method with 6-311++ G** basis set are shown in Table 1.

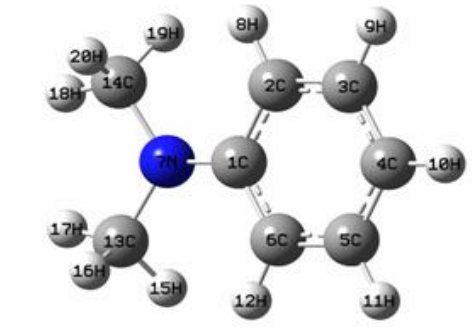

Fig. 1. The optimized molecular structure of NNDMA

Table 1. Total energies of NNDMA, calculated at DFT (B3LYP)/6-31G* and (B3LYP)/6-311+G level**

Method	Energies (Hartrees)
6-31G*	-366.19569865
6-311+G**	-366.21545485

Assignments of spectra

The optimized geometrical parameters obtained by the large basis set calculation were presented in Table 2. A detailed description of vibrational modes can be given by means of normal coordinate analysis. For this purpose, a full set of 68 standard internal coordinates containing 14 redundancies were defined as given in Table 3. From these, a non–redundant set of local symmetry coordinates were constructed by suitable linear combinations of internal coordinates following the recommendation of Pulay *et al* [4,5] and they are presented in Table 4. The theoretically calculated DFT force fields were transformed to this later set of vibrational coordinates and used in all subsequent calculations.

The observed and calculated wave numbers and normal mode descriptions for the title compound are reported in Table 5. When using computational methods to predict theoretical normal vibrations for relatively complex polyatomic, scaling strategies are used bring computed wave numbers. For the DFT method employed in this work the simplest limiting scaling strategy was used.

In order to reproduce the observed wave numbers, refinement of scaling factors were applied and optimized via least-square refinement algorithm which resulted is an average difference between the experimental and SQM wave numbers for 6-311++G** basis set. The vibrational assignments in the present work are based on the DFT/6-311++G** frequencies, Infrared intensities, Raman activities as well as characteristic group frequencies. The 54 normal modes of NNDMA are distributed among the symmetry species as √vib=37A'(in-plane)+17A" (out-of-plane). The detailed vibrational assignments of fundamental modes of NNDMA have been reported in Table 5. Assignments were made through visualization of the atomic displacement representations for each vibration, viewed through GAUSSVIEW [6] and matching the predicted normal wave numbers and intensities with experimental data.

Table 2. Optimized geometrical parameters of NNDMA obtained by B3LYP/ 6–311+G density functional calculations**

Bond length	Value(Å)	Bond angle	Value(Å)	Dihedral angle	Value(Å)
C2-C1	1.38599	C3-C2-C1	120.00023	C4-C3-C2-C1	0.00000
C3-C2	1.38610	C4-C3-C2	120.00023	C5-C4-C3-C2	0.00000
C4-C3	1.38599	C5-C4-C3	119.99953	C6-C1-C2-C3	0.00000
C5-C4	1.38599	C6-C1-C2	119.99953	N7-C1-C2-C3	179.42348
C6-C1	1.38599	N7-C1-C2	119.99897	H8-C2-C1-N7	-1.14850
N7-C1	1.44595	H8-C2-C1	120.00345	H9-C3-C4-C5	-179.42800
H8-C2	1.12200	H9-C3-C4	120.00345	H10-C4-C5-C6	-179.42800
H9-C3	1.12200	H10-C4-C5	119.99899	H11-C5-C6-C1	-179.42806
H10-C4	1.12194	H11-C5-C6	119.99384	H12-C6-C1-N7	1.14850
H11-C5	1.12200	H12-C6-C1	120.00345	C13-N7-C1-C2	121.14512
H12-C6	1.12200	C13-N7-C1	119.99802	C14-N7-C1-C2	-59.42066
C13-N7	1.44600	C14-N7-C1	120.00317	H15-C13-N7-C1	-59.92235
C14-N7	1.44596	H15-C13-N7	109.49954	H16-C13-N7-C1	59.92916
H15-C13	1.12200	H16-C13-N7	109.49858	H17-C13-N7-C1	-180.00000
H16-C13	1.12201	H17-C13-N7	109.50516	H18-C14-N7-C1	-180.00000
H17-C13	1.12193	H18-C14-N7	109.49847	H19-C14-N7-C1	59.92122
H18-C14	1.12200	H19- C14-N7	109.50412	H20-C14-N7-C1	-59.93417
H19-C14	1.12192	H20- C14-N7	109.49473		
H20-C14	1.12201				

*for numbering of atom refer Fig. 1

Table 3. Definition of internal coordinates of NNDMA

No(i)	symbol	Type	Definition
Streching 1-6	r_i	C-C(ring)	C1-C2,C2-C3,C3-C4,C4-C5,C5-C6,C6-C1
7-11	R_i	C-H(aro)	C2-H8,C3-H9,C4-H10,C5-H11,C6-H12
12-14	S_i	C-N (sub)	C1-N7, N7-C14,N7-C13
15-17	s_i	C-H(f)(methyl)	C14-H18,C14-H19,C14-H20
18-20	P_i	C-H(s)(methyl)	C13-H15,C13-H16,C13-H17
Bending 21-26	α_i	C-C-C(ring)	C1-C2-C3,C2-C3-C4,C3-C4-C5, C4-C5-C6,C5-C6-C1,C6-C1-C2
27-36	θ_i	C-C-H	C1-C2-H8,C3-C2-H8, C2-C3-H9,C4-C3-H9,C3-C4-H10, C5-C4-H10,C4-C5-H11,C6-C5-H11,C5-C6-H12,C1-C6-H12
37-40	β_i	C-C-N	C6-C1-N7,C2-C1-N7,C14-N7-C1,C13-N7-C1
41-43	n_i	H-C-H(f)(methyl)	H18-C14-H19,H19-C14-H20,H20-C14-H18
44-46	γ_i	N-C-H(f)(methyl)	N7-C14-H18,N7-C14-H19,N7-C14-H20
47-49	ρ_i	H-C-H(s)(methyl)	H15-C13-H16,H16-C13-H17,H17-C13-H15
50-52	Φ_i	N-C-H(s)(methyl)	N7-C13-H15,N7-C13-H16,N7-C13-H17
Out-of-plane 53-57	ω_i	C-C-H	H8-C2-C1-C3,H9-C3-C2-C4,H10-C4-C3-C5, H11-C5-C4-C6,H12-C6-C5-C1
58	μ_i	C-C-N	N7-C1-C6-C2
Torison 59-60	τ_i	τC-N	C14-N7-C1-C6(C2),C13-N7-C1-C6(C2)
61-66	τ_i	τring	C1-C2-C3-C4,C2-C3-C4-C5, C3-C4-C5-C6,C4-C5-C6-C1, C5-C6-C1-C2,C6-C1-C2-C3
67-68	τ_i	τC-H(methyl)/3	C1-N7-C14(H18,H19,H20), C1-N7-C13(H15,H16,H17)

*for numbering of atom refer Fig. 1

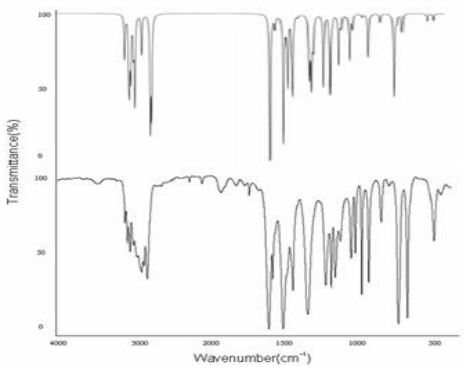

Fig. 2 FT-IR spectra of NNDMA
(a)Observed (b) Calculated with B3LYP/6-311+G**

Table 4. Definition of local symmetry coordinates and the value corresponding scale factors used to correct the force fields for NNDMA

No.(i)	Symbol[a]	Definition[b]	Scale factors used in calculation
1-6	C-C(ring)	r1,r2,r3,r4,r5,r6	0.963
7-11	C-H(aro)	R7,R8,R9,R10,R11	0.916
12-14	C-N(sub)	S12,S13,S14	0.916
15	CH_3ssf	(s15+s16+s17)/ √3	0.995
16	CH_3ipsf	(2s16-s15-s17)/ √6	0.992
17	CH_3opsf	(s15-s17)/ √2	0.919
18	CH_3sss	(P18+P19+P20)/ √3	0.995
19	CH_3ipss	(2P19-P18-P20)/ √6	0.992
20	CH_3opss	(P18-P20)/ √2	0.919
21	bring	(α21-α22+α23-α24+α25-α26)/ √6	0.992
22	bring	(2α21-α22-α23+2α24-α25-α26)/ √12	0.992
23	bring	(α22-α23+α25-α26)/2	0.992
24-28	C-C-H	(θ27-θ28) /√2,(θ29-θ30) /√2, (θ31-θ32) /√2,(θ33-θ34) /√2, (θ36-θ36) /√2	0.923
29-31	C-C-N	(β37-β38) /√2, β39, β40	0.967
32	CH_3sbf	(n41+n42+n43-γ44-γ45-γ46)/ √6	0.990
33	CH_3ipbf	(2n43-n41-n42)/ √6	0.990
34	CH_3opbf	(n41-n43)/ √2	0.990
35	CH_3iprf	(2γ45-γ44-γ46)/ √6	0.990
36	CH_3oprf	(γ44-γ46)/ √2	0.990
37	CH_3sbs	(ρ47+ρ48+ρ49-Φ50-Φ51-Φ52)/ √6	0.990
38	CH_3ipbs	(2ρ49-ρ47-ρ48)/ √6	0.990
39	CH_3opbs	(ρ47-ρ49)/ √2	0.990
40	CH_3iprs	(2Φ51-Φ50-Φ52)/ √6	0.990
41	CH_3oprs	(Φ50-Φ52)/ √2	0.990
42-46	C-C-H	ω53, ω54, ω55, ω56, ω57	0.994
47	C-C-N	μ58	0.962
48-49	C-N	τ59, τ60	0.830
50	tring	(τ61-τ62+τ63-τ64+τ65-τ66)/√6	0.994
51	tring	(τ61-τ63+τ64-τ66)/2	0.994
52	tring	(-τ61+2τ62-τ63-τ64+2τ65-τ66)/√12	0.994
53	τC-H(f)	τ67/3	0.979
54	τC-H(s)	τ68/3	0.979

a These symbols are used for description of the normal modes by TED in Table 5.
b The internal coordinates used here are defined in Table 3.

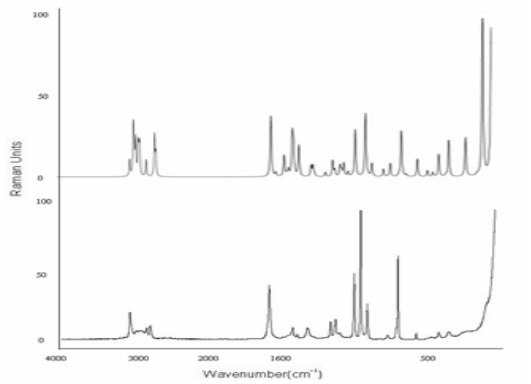

Fig. 3 FT-Raman spectra of NNDMA
(a) Observed (b) Calculated with B3LYP/6-311+G**

C-C vibrations

The bands between 1400–1650 cm^{-1} in benzene derivatives are assigned to C-C stretching modes [7]. Accordingly, in the present study, the carbon-carbon vibrations of the title compound are observed at 1509, 1577 and 1578 cm^{-1} in the FT-IR spectrum and 1520 cm^{-1} in the FT-Raman.

C-H vibrations

The aromatic structure shows the presence of C–H stretching vibrations around 3000 cm^{-1}. In NNDMA these modes were observed at 3074, 3063, 3027, 2984 and 2996 cm^{-1}. A number of spikes observed throughout the broad absorption is indicative of Fermi resonance. In benzene-like molecule C–H in-plane bending vibrations are observed in the region 1000–1300 cm^{-1} and are usually weak. The C–H out-of-plane bending modes arise in the region 600–900 cm^{-1} [8]. In the present study, the bands observed at 1168, 1231, 1216 and 1360 cm^{-1} in NNDMA were assigned to C–H in-plane bending vibrations. The C–H out-of-plane bending modes for NNDMA are also assigned within characteristic region and were presented in Table 5.

Ring vibrations

Due to aromatic ring vibrations, NNDMA absorb strongly in the region 1635–1300 cm^{-1} [9,10]. In the present study the peaks observed at 1672, 1637, 1578, 1558, 1500, 1472, 1444, 1385 and 1372 cm^{-1} were assigned to ring stretching vibrations. The ring deformation vibrations were observed at 1131, 704, 554, 516, 473 and 288 cm^{-1} for NNDMA. For most of the remaining ring vibrations, the overall agreement is satisfactory. Small changes in frequencies observed for these modes are due to the changes in force constant/reduced mass ratio resulting mainly due to the extents of mixing between ring and substituent group vibrations.

Carbon–nitrogen vibration

The IR and Raman bands observed between 1444 and 1229 cm^{-1}, in the title compounds have been assigned to C-N stretching vibrations [11]. The in-plane and out-of-plane bending vibrations assigned in this study are also supported by the literature [12]. For the title compounds a pure mode cannot be expected for this vibration since it falls in a complicated region of the vibrational spectrum.

CH_3 vibration

The CH_3 stretching and bending modes appear to be quite pure group vibrations. Considering the assignment of CH_3 group frequencies, one can expect that nine fundamentals and can be associated to each CH_3 group, namely the symmetrical $\nu_s(CH_3)$, and asymmetrical $\nu_a(CH_3)$, in-plane stretching modes; the symmetrical $\alpha_s(CH_3)$ and asymmetrical $\alpha_a(CH_3)$, deformation modes; the in-plane rocking and out-of-plane rocking and twisting bending modes. The asymmetric stretching and asymmetric deformation modes of the methyl group is expected to be depolarised for $A^{'}$ symmetry species. The infrared bands observed at 2804 cm^{-1} is assigned to $\nu s(CH_3)$. The FT-IR in plane bending and Raman out-of-plane bending are assigned to 1229, 1195 cm^{-1}, respectively. The assignment of the band at 282 cm^{-1} of IR is attributed to the torsion CH_3 [13].

Hyperpolarizability calculation

For calculating the hyperpolarizability, The optimization has been carried out in the unrestricted open-shell Hartree-Fock level. The geometries are fully optimized without any constraint with the help of analytical gradient procedure implemented within Gaussain 03W program [14]. The electric dipole moment and dispersion free first-order hyperpolarizability are calculated using finite field method. The finite field method offers a straight forward approach to the calculation of hyperpolarizability. The 3-21(d,p) basis set gives remarkably good geometries for such a small basis set and infact it is used for the geometry optimization of some high accuracy energy methods.

The nonlinear properties of an isolated molecule in an electric field $E_i(\omega)$ can be represented by the Taylor expansion of the total dipole moment mi induced by the field
Taken at zero field,

Dipole moment $\mu_i = -\left[\frac{\partial^2 E}{\partial F_i \partial F_j}\right]_0$

Components of polarizability tensor:

$$\alpha_{ij} = -\left[\frac{\partial E}{\partial F_i}\right]_0$$

Components of hyperpolarizability tensor:

$$\beta_{ijk} = -\left[\frac{\partial^3 E}{\partial F_i \partial F_j \partial F_k}\right]_0$$

These components are to be distorted by an external electric field. The value of total static polarizability and hyperpolarizability are obtained from the following equation,

$$\beta_{tot} = [(\beta_{xxx} + \beta_{xyy} + \beta_{xzz})^2 + (\beta_{yyy} + \beta_{yzz} + \beta_{yxx})^2 + (\beta_{zzz} + \beta_{zxx} + \beta_{zyy})^2]^{1/2}$$

In the presence of an applied electric field, first order hyperpolarizability is a third rank tensor that can be described by a 3×3×3 matrix. The components of the 3D matrix can be reduced to 10 components because of the Kleinman symmetry [15]. The matrix can be given in the lower tetrahedral format. It is obvious that the lower part of the 3×3×3 matrix is a tetrahedral. The calculation of NLO properties with high accuracy is challenging and requires consideration of many different issues. Computational techniques are becoming valuable in designing, modeling and screening novel NLO materials. The calculated value of hyperpolarizability for the title compound is 0.402499×10^{-30} esu, which is nearly 2 times that of urea (0.1947×10^{-30} esu). The calculated values of dipole moment and hyperpolarizability values are tabulated in Table 6. The β_{zxx} direction shows biggest value of hyperpolarizability which insists that the delocalization of electron cloud is more that direction than other directions.

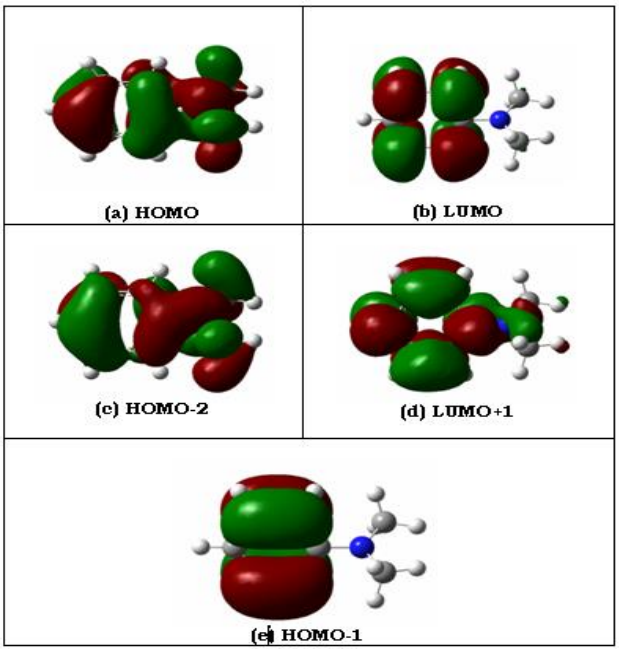

Fig. 4. Representation of the orbital involved in the electronic transition for (a) HOMO (b) LUMO (c) HOMO-2 (d) LUMO+1 (e) HOMO-1

The static polarizability value [16-17] is proportional to the optical intensity and inversely proportional to the cube of transition energy. With this concept, larger oscillator strength (f_n) and $\Delta\mu_{gn}$ with lower transition energy (E_{gn}) is favourable to obtain large first static polarizability values. Electronic excitation energies, oscillator strength and nature of the respective excited states were calculated by the closed-shell singlet calculation method and are summarized in Table 7. Orbital involved in the electronic transition for (a) HOMO (b) LUMO (c) HOMO-2 (d) LUMO+1 (e) HOMO-1 is represented in Fig. 4. The Fig. 4a and Fig. 4b shows the highest occupied molecule orbital (HOMO) and lowest unoccupied molecule orbital (LUMO) of NNDMA. There is an inverse relationship between hyperpolarizability and HOMO–LUMO. The NLO responses can be understood by examining the energetic of frontier molecular orbitals. There is an inverse relationship between hyperpolarizability and HOMO–LUMO.

HOMO energy =−0.296 a.u

LUMO energy = 0.148 a.u

HOMO–LUMO energy gap = 0.444 a.u

Table 6. The dipole moment (μ) and first-order hyperpolarizibility (β) of NNDMA derived from DFT calculations

β_{xxx}	0.46927
β_{xxy}	-0.11436
β_{xyy}	-0.27422
β_{yyy}	-0.00713
β_{zxx}	0.205357
β_{xyz}	0.072191
β_{zyy}	-0.15792
β_{xzz}	0.155044
β_{yzz}	0.129833
β_{zzz}	0.15098
β_{total}	0.402499
μ_x	0.02525878
μ_y	6.1127E-05
μ_z	0.00874343
μ	0.18456254

Dipole moment (μ) in Debye, hyperpolarizibility β(-2ω; ω,ω) 10^{-30}esu.

Table 7.Computed absorption wavelength (λ_{ng}) , energy (E_{ng}), oscillator strength (f_n) and its major contribution.

n	λ_{ng}	E_{ng}	f_n	Major contribution
1	163.4	7.59	0.0073	H-0->L+0(+47%), H-1->L+1(37%), H-2->L+0(+13%)
2	161.1	7.70	0.1203	H-0->L+1(+78%), H-1->L+0(+12%)
3	140.3	8.84	0.0786	H-2->L+1(+46%), H-1->L+0(+38%)

(Assignment; H=HOMO,L=LUMO,L+1=LUMO+1,etc.)

Conclusions

IR and Raman Spectra were obtained for NNDMA, in which all of the expected 54 normal modes of vibration were assigned. The optimized molecular geometry, force constants and vibrational frequencies were calculated using DFT techniques in the B3LYP approximation. Taking the observed

frequencies as a basis corresponding to the fundamental vibrations, it was possible to proceed to a scaling of the theoretical force field. The resulting SQM force field served to calculate the potential energy distribution, which revealed the physical nature of the molecular vibrations, and the force constants in internal coordinates, which were similar to the values obtained before for related chemical species. The first-order hyperpolarizibility (β_{ijk}) of the novel molecular system of NNDMA is calculated using 3-21 G (d,p) basis set based on finite field approach. The calculated first-order hyperpolarizability (β_{total}) of NNDMA is 0.402499×10^{-30} esu, which is nearly 2 times greater than that of urea (0.1947×10^{-30} esu). Electronic excitation energies, oscillator strength and nature of the respective excited states were calculated by the closed-shell singlet calculation method. Such a material could provide for a new impulse in the field of second-order nonlinear optical materials.

Table 5. Detailed assignments of fundamental vibrations of NNDMA by normal mode analysis based on SQM force field calculation

S. No.	Symmetry species C_s	Observed frequency (cm^{-1})		Calculated frequency (cm^{-1}) with B3LYP/6-311+G ** force field				TED (%) among type of internal coordinates[c]
		Infrared	Raman	Unscaled	Scaled	IR[a] A_i	Raman[b] I_i	
1	A'	3231		3335	3228	29.116	73.18	CH(94)
2	A'		3195	3199	3193	5.777	200.999	CH(97)
3	A'	3191		3196	3192	26.273	18.243	CH(98)
4	A'		3186	3195	3184	39.932	63.51	CH3ips(85),CH3sss(7),CH3ops(5)
5	A'	3173		3179	3172	37.568	147.222	CH(99)
6	A'	3152		3156	3149	20.768	113.612	CH(99)
7	A'	3140		3149	3143	5.142	60.649	CH(99)
8	A'		3132	3142	3135	57.315	120.485	CH3ssf(86),CH3ops(11)
9	A'	3063		3080	3074	26.399	63.75	CH3ops(90),CH3ips(8)
10	A'		2993	3001	2996	71.539	145.149	CH3sss(86),CH3ips(6)
11	A'		2981	2991	2984	61.845	78.218	CH3ops(79),CH3ssf(14)
12	A'			1678	1672	104.66	56.828	CC(68),bCCH(19),bring(9)
13	A'		1635	1643	1637	8.507	3.523	CC(67),bCCH(15),bCCN(9),bring(9)
14	A'	1577		1585	1578	84.122	17.74	bCH3op(51),bCH3ip(23),bCH3ip(11),bCH3op(8)
15	A'		1557	1565	1558	4.059	2.57	bCH3op(41),bCH3ip(35),bCH3ip(8),bCH3op(6)
16	A'			1553	1547	45.405	5.426	bCH3op(23),bCCH(21),bCH3ip(17),CC(15),bCH3sb(6)
17	A'	1518		1526	1519	10.727	30.261	bCH3op(42),bCH3ip(32),bCH3ip(16),bCH3op(7)
18	A'		1512	1519	1512	11.878	12.54	bCH3ip(43),bCH3op(21),bCH3op(19),bCH3ip(14)
19	A'	1509		1520	1511	38.853	10.351	bCH3op(29),bCH3sb(25),bCH3ip(20),bCH3sb(10),bCCH(9)
20	A'		1500	1510	1500	1.33	0.701	bCCH(38),CC(35),bCCN(12),bCH3sb(7)
21	A'	1474		1478	1472	1.463	23.083	bCH3sb(56),bCH3sb(30)
22	A'	1386		1390	1385	38.356	7.264	CC(37),CN(16),bCH3op(14),bCH3op(12),bCCN(11)
23	A'		1371	1378	1372	44.479	7.009	CC(54),bCCH(15),CN(12)
24	A'		1362	1368	1360	18.453	2.116	bCCH(63),bCCN(16),CN(11)
25	A'	1283		1289	1282	48.041	2.701	CN(28),CC(24),bCH3op(14),bCCH(12),bCH3op(7)
26	A'	1229		1237	1231	52.66	8.823	bCH3op(27),CN(27),CC(13),bCCH(10),bCH3op(9),bring(8)
27	A'		1214	1224	1216	3.237	3.637	bCCH(79),CC(17)
28	A'		1175	1184	1178	1.031	5.579	bCCH(90),CC(9)
29	A'	1167	1161	1175	1168	32.924	2.951	bCH3ip(40),bCH3op(12),bCH3ip(9),CN(9),bCH3ip(7),bCH3op(6)
30	A'			1159	1151	7.387	6.631	bCH3ip(27),bCH3ip(25),bCH3op(15),bCH3op(9),bCH3ip(6),bCH3ip(6)
31	A'	1131		1126	1120	1.333	2.251	CC(46),bCCH(42),bCCN(5)
32	A'	1092	1090	1097	1091	30.274	0.385	CN(37),bCH3ip(27),bCH3op(8),bCH3ip(6)
33	A"	1070		1076	1070	9.186	20.676	CC(73),bCCH(22)
34	A"	991	993	1003	997	2.294	24.997	bring(69),CC(29)
35	A"	981		985	978	0.37	0.69	gCCH(86),tring(14)
36	A'		950	956	951	28.305	3.884	CN(54),CC(17),bring(11)
37	A"	945	948	959	949	0.471	1.117	gCCH(91),tring(8)
38	A"			874	868	5.683	2.472	gCCH(77),tring(14),gCCN(8)
39	A"	813		829	820	0.009	3.998	gCCH(98)
40	A"		759	766	760	54.764	0.501	gCCH(52),tring(28),gCCN(17)
41	A'	750	743	745	740	4.2	11.769	CN(43),bring(38),CC(12)
42	A"			710	704	12.031	0.548	tring(66),gCCH(26),gCCN(7)
43	A'		623	635	626	0.038	3.588	bring(85),bCCH(5),CC(5)
44	A'	556	550	562	554	0.097	1.052	bring(37),bCCN(37),CN(9)
45	A"	514		523	516	5.139	0.685	tring(40),gCCN(33),gCCH(18)
46	A'		471	478	473	4.634	2.988	bCCN(84),CC(6)
47	A"		428	430	425	0.099	0.174	tring(79),gCCH(19)
48	A"		401	409	402	0.465	3.822	bring(29),CN(25),bCCN(22),CC(7),tCH3f(5)
49	A"		287	295	288	0.23	0.082	bCCN(57),tCH3f(15),tCH3s(11)
50	A"		286	289	282	3.752	2.33	tring(31),bCCN(19),tCH3s(16),tCH3f(15),tCN(9),gCCH(7)
51	A"		203	210	200	0.023	0.061	bCCN(36),tCH3f(28),tCH3s(27)
52	A"		162	167	161	0.968	4.015	tring(35),tCH3s(22),tCH3f(21),tCN(6)
53	A"		103	109	101	8.631	1.427	tCN(53),bCCN(29),CN(7)
54	A"			75	67	0.004	2.329	tCN(68),tCH3f(13),tCH3s(13)

Abbreviations used: b, bending; g, wagging; t, torsion; s, strong; vs, very strong; w, weak; vw, very weak;

[a] Relative absorption intensities normalized with highest peak absorption

[b] Relative Raman intensities calculated by Eq.1 and normalized to 100.

[c] For the notations used see Table 4.

References

[1] B.A.Hess Jr., J. Schaad, P.Carsky, R.Zahradnik, Chem. Rev., 86 (1986) 709.
[2] P.Pulay, X.Zhon, G.Fogarasi, in : R. Fransto (Ed), NATO ASI series, Vol C 406, Kluwer, Dordrecht, 1993.
[3] C. Lee, W. Yang, R.G. Parr, Phys. Rev., B37 (1988) 785.
[4] P. Pulaaay, G. Fogarasi, G.Pongor, J. E. Boggs, A. Vargha, J. Am. Chem. Soc., 105 (1983) 7037.
[5] G. Fogarasi and P. Pulay In: J.R. Durig, Editor, Vibrational Spectra and Structure vol. 14, Elsevier, Amsterdam (1985), p. 125.
[6] A. Frisch, A.B. Nielson and A.J. Holder, Gaussview Users Mannual, Gaussian Inc., Pittsburgh, PA (2000).
[7] D.N. Sathyanarayana, Vibrational Spectroscopy, Theory and Applications, New Age International Publishers, New Delhi, 2004.
[8] W.O. George, P.S. Cintyne, in: D.J. Mowthrope (Ed.), Infrared Spectroscopy, John Wiley & Sons, UK, 1987.
[9] T. Sundius, Vib. Spectrosc. 29 (2002) 89.
[10] Molvib (V.7.0), Calculation of Harmonic Force Fields and Vibrational Moles of Molecules, QCPE Program No. 807, 2002.
[11] L.J. Bellamy, Advances in Infrared group frequencies, Barnes and Noble Inc., USA, 1968.
[12] V. Krishnakumar, R. John Xavier, Chem. Phys. Chem. Phys. 312 (2005)
227.
[13] S.J. Bunce, H.G. Edwards, A.F. Johnson, I.R. Lewis, P.H. Turner, Spectrochim. Acta, 49 A (1993) 775.
[14] A. Frisch, A.B. Nielson and A.J. Holder, Gaussview Users Mannual, Gaussian Inc., Pittsburgh, PA (2000).
[15] D.A. Kleinman, Phys. Rev. 1962;126,1977.
[16] K. Wu, C. Liu, C. Mang, Opt. Mater. 29 (2007) 1129–1137.
[17]S. Iran, W.M.F. Fabian, Dyes Pigments 70 (2006) 91–96.